

《Original》

## Sensitivity Analysis on PWR Reactivity Induced Accidents

Myung Hyun Kim and Un Chul Lee  
Seoul National University

Ki In Han  
Korea Advanced Energy Research Institute  
(Received June 17, 1982)

### 가압경수로 반응도사고에 대한 민감도 분석

김 명 현 · 이 은 철

서울대학교

한 기 인

한국에너지연구소

(1982. 6. 17 접수)

#### Abstract

Analyzed is the sensitivity of reactor transient behavior to various reactor parameters during the reactivity induced accidents (RIA) of the Kori Unit 1. Included in the analysis is a partial spectrum of RIAs with relatively fast transients such as uncontrolled rod cluster control assembly bank withdrawal from a subcritical or low power startup condition and rod ejection accidents.

The analysis can be performed generally in three steps; calculation of an average core power change, hot spot heat transfer calculation and DNBR (departure from nucleate boiling ratio) calculation. The computer codes used for the analysis are either developed based on the codes relevant to it. These codes are evaluated to be highly reliable.

An extensive sensitivity analysis is performed to study the effects of various reactor design and operating parameters on the reactor transient behavior during the accidents. The assumptions and initial conditions used for the RIA analysis in the Kori Unit 1 FSAR (Final Safety Analysis Report) are reexamined, and the corresponding analysis results are reassessed, based on the sensitivity analysis results, to be conservative and reliable.

#### 요 약

고리 1호기 일부 반응도사고에 대한 민감도 분석을 수행하였다. 본 민감도 분석에 고려한 반응도 사고는 비교적 진행속도가 빠른 사고로서 미임계나 저출력 시동조건에서 발생한 제어뱅크 인출사고와 제어봉 인출사고가 이에 속한다.

본 분석작업은 다음과 같이 세 단계로 수행하는 바 원자로 평균출력의 변동 계산과 최고점에서의 열전달계산 그리고 DNBR계산 단계로 나눌 수 있다. 계산에 사용된 계산코드들은 본 분석을 위하여

개발하거나 기존 전산코드들을 수정·보완하여 제작하였으며 신뢰도도 평가하였다.

원자로 설계 및 운전변수들이 사고발생시 원자로의 거동에 미치는 영향을 조사하기 위하여 민감도 분석을 수행하였다.

본 민감도 분석 결과에 근거하여 고리 1호기 반응도사고 분석에 사용된 최종안전분석보고서의 가정과 초기조건이 타당한가를 조사하였고, 또한 계산 결과도 보수적이고 신뢰할수 있는지 판별하였다. 고리 1호기 반응도사고 분석에 사용된 가정 및 초기조건을 재검토하고 민감도를 분석한 결과 최종안전분석보고서의 해석결과는 보수적이고 신뢰할 수 있는 것으로 평가되었다.

### Nomenclature

$D_i^1$ :	fast neutron diffusion coefficient at node $i$
$D_i^2$ :	thermal neutron diffusion coefficient at node $i$
$\phi_i^1$ :	fast neutron flux at node $i$
$\phi_i^2$ :	thermal neutron flux at node $i$
$\Sigma_{ri}$ :	macroscopic removal cross-section at node $i$
$\Sigma_{ai}^1$ :	macroscopic fast neutron absorption cross-section at node $i$
$\Sigma_{fi}^2$ :	macroscopic thermal neutron absorption cross-section at node $i$
$\Sigma_{fi}^1$ :	macroscopic fast neutron fission cross-section at node $i$
$\Sigma_{fi}^2$ :	macroscopic thermal neutron fission cross-section at node $i$
$\beta_k$ :	delayed neutron yield fraction from precursor group $k$
$\beta_{eff}$ :	effective delayed neutron yield fraction
$\nu$ :	the number of neutrons per fission
$v^1$ :	fast neutron velocity
$v^2$ :	thermal neutron velocity
$C_{ki}$ :	precursor concentration for delayed group $k$ at node $i$
$\lambda_k$ :	decay constant for delayed group $k$
$\Delta t$ :	time increment

## 1. Introduction

Reactivity induced accident is defined as an incident caused by an excessive reactivity insertion into reactor core leading to a mismatch between heat generation and cooling within the core. Such an excessive reactivity insertion can be caused by rod cluster control assembly withdrawal, rod ejection, boron dilution or an addition of cold water to the reactor coolant system. In such incidents, reactor power may rise to a level beyond which the normal heat removal capability is not sufficient for effective reactor core cooling.

The objectives of the reactivity induced accident analysis are to look into the reactor core behavior during such accidents and to assure the safety of the plant. The reactivity induced accidents are characterized by the rate of reactivity insertion and the extent of power mismatch. The consequence of the accident is also largely dependent on the reactor condition and the severity of the initiating event.

Among the full spectrum of postulated reactivity induced accidents, studied herein are the relatively fast transients called superprompt critical excursions such as uncontrolled rod cluster control assembly bank withdrawal from a subcritical or low power startup condition and rod ejection accidents. During such fast transients, response from the loop can be neglected due to the longer loop transit time compared to the reactor core response time, and a simulation of the overall reactor system including steam generators, pumps and loops is not required in the analysis. The analysis can be performed generally in three steps; calculation of an average core power change, hot spot heat transfer calculation and DNBR calculation. The required computer codes are either developed or adapted at KAERI for the calculation.

An extensive sensitivity analysis is performed to study the effects of various reactor design and operating parameters on the reactor transient behavior during the accidents. A reference case for the accident, that serves the basis for the sensitivity analysis, adopts the assumptions and initial conditions used in the Kori Unit 1 FS-

AR<sup>1)</sup>. The assumptions and initial conditions used for the reference case are examined, based on the sensitivity analysis results, to study if the FSAR values are conservative and acceptable forming the bounding values.

## 2. Brief Description of Accidents

### 2.1. Uncontrolled Rod Cluster Control Assembly Bank Withdrawl from a Subcritical or Low Power Startup Condition

This accident could occur due to a reactor control system malfunction which causes the rod control mechanisms to force a rod withdrawal even in the absence of an operator initiated control signal. This could happen either at subcritical, hot shutdown or start-up condition. This is categorized as the ANS condition II even.

Because this accident is initiated from a low power level, sufficient reactivity is inserted to exceed prompt critical condition before the power level rises to a high level enough either to cause a flux trip or to result in significant temperature feedback. Once prompt critical condition is exceeded, the rate of power increase is so rapid that the reactor can become subcritical only by the prompt negative reactivity feedback from the rising fuel temperature before the flux trip becomes effective. Although the peak power is very high, the power burst is so narrow that the total energy released in the fuel in this particular excursion is not sufficient to cause fuel damage.

### 2.2. Rod Ejection Accident

For the postulated control rod ejection accident, a mechanical failure of a control rod housing is assumed such that the control rod and drive shaft is ejected to the fully withdrawn position due to the reactor coolant system pressure. The consequences of this mechanical failure induce

a rapid reactivity insertion together with an adverse core power distribution. This incident may result in damage to a considerable number of fuel rods and release of fission products to the coolant. However, it should be assured that the rest of the primary pressure boundary is not breached, and that the radioactivity release is limited to a small amount.

The clad failure mechanism appears to be melting for unirradiated rods and brittle fracture for irradiated rods. Also, important is the conversion ratio of thermal to mechanical energy in the fuel rod. The conversion ratio depends on the maximum stored energy in the fuel. This accident is categorized as a design-basis accident and belongs to ANS condition IV event.

## 3. Methods of Analysis

The reactivity induced accidents are generally analyzed in three steps; an average core nuclear power transient calculation, hot spot heat transfer calculation, and DNBR calculation. Shown in Figure 1 are the general analysis procedure and corresponding computer codes utilized.

### 3.1. Average Core Nuclear Power Transient Calculation

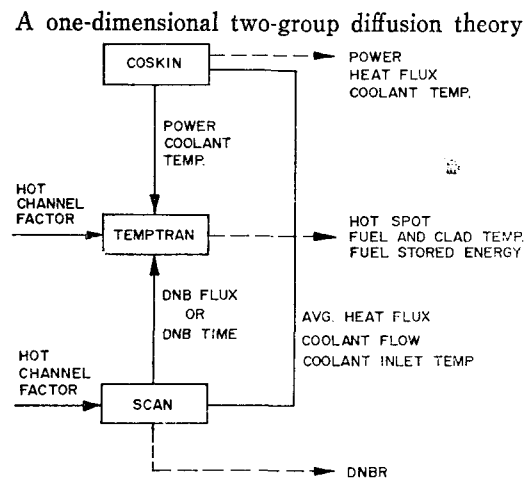


Fig. 1. RIA Analysis Procedure and Related Computer Codes.

code, COSKIN is employed for the calculation of an average core nuclear power transient.

The COSKIN code is developed based on COSTAX-BOIL<sup>2)</sup> that includes numerous trip functions and updated core thermal calculation routines. The code solves two-group neutron diffusion theory kinetics equations with six delayed neutron groups. Kinetic equations are solved by implicit finite difference backward algorithm. The code includes a detailed multi-region transient heat transfer model for calculation of pointwise doppler and moderator feedback effects. It allows a more realistic representation of the spatial effects of axial moderator feedback and rod cluster control assembly movement than the point kinetics model.

The two-group time dependent diffusion theory equations for each spatial node  $i$  are written as:

$$\begin{aligned} \nabla \cdot D_i^1 \nabla \phi_i^1 - [\sum_{r_i} + \sum_{a_i}^1] \phi_i^1 + (1 - \beta_{eff}) \\ [\nu \sum_{f_i}^1 \phi_i^1 + \nu \sum_{f_i}^2 \phi_i^2] + \sum_k \lambda_k C_{ki} \\ - \frac{1}{\nu^1 \Delta t} \phi_i^1 = - \frac{1}{\nu^1 \Delta t} \phi_i^{1*} \\ \nabla \cdot D_i^2 \nabla \phi_i^2 - \sum_{a_i}^2 \phi_i^2 + \sum_{r_i} \phi_i^1 - \frac{1}{\nu^2 \Delta t} \phi_i^2 \\ = - \frac{1}{\nu^2 \Delta t} \phi_i^{2*} \\ C^{ki} = \frac{C_{ki}^*}{1 + \lambda_k \Delta t} + \frac{\Delta t \beta_k}{1 + \lambda_k \Delta t} [\nu \sum_{f_i}^1 \phi_i^{1*} + \nu \sum_{f_i}^2 \phi_i^{2*}], \end{aligned}$$

where  $C_{ki}^*$  and  $\phi_i^{k*}$  are delayed neutron precursor density of group  $k$  and neutron flux at previous time step, respectively. Group constants in the above equations are obtained from burnup dependent diffusion theory code.

### 3.2. Hot spot Heat Transfer Calculation

The hot spot heat transfer analysis is performed using the detailed fuel and clad transient heat transfer computer code, TEMPTRAN<sup>3)</sup>, which is developed based on the calculational logics of the FACTRAN code<sup>4)</sup>. The TEMPTRAN code calculates the transient temperature distribution in a cross section of a metal-clad UO<sub>2</sub>-fuel rod and the heat flux at the surface

of the rod using input data like nuclear power versus time and the local coolant conditions at the hot channel. The zirconium-water reaction is explicitly represented, and all material properties are represented as functions of temperature.

### 3.3. DNBR Calculation

For the hot channel DNB analysis, one-dimensional single channel thermal-hydraulic DNB analysis code, SCAN<sup>5)</sup>, is adopted, in which the W-3 DNB correlation is utilized.

The basic assumption included in the SCAN code is that a single channel analysis result can be made comparable to (with reasonable accuracy) the DNBR result of multi-channel analysis by matching local coolant condition through the use of bias curve. Bias curve accounts for the effects of flow redistribution and thermal mixing on hot channel, mass velocity and enthalpy rise. Since a single channel analysis cannot directly obtain these effects, they must be determined from other sources like experimental results or computer code calculation results.

## 4. General Assumptions and Calculational Models

### 4.1. Reactivity Insertion

During reactor operation, control rod insertion is limited to assure adequate trip reactivity available to meet the power distribution requirement and to limit the consequences of a hypothetical rod ejection accident. The available shutdown reactivity decreases with the reduction in boron concentration in the coolant, for the power and temperature defects are the largest at the minimum boron concentration condition.

For the analysis of control bank withdrawal accident, the maximum positive reactivity insertion rate is assumed to be higher than that with the simultaneous withdrawal of the two

control banks having the greatest combined worth at their maximum speeds (45 inches/min). This rate (75pcm/sec) is also higher than the maximum rate of reactivity increase during boron dilution accident.

#### 4.2. Feedback Model

Pointwise doppler feedback and moderator temperature feedback models are considered. Since the magnitude of the peak power during the transient for any given rate of reactivity insertion is strongly dependent on the doppler coefficient, a conservative value (minimum absolute magnitude) is chosen as a constant to yield the maximum peak power.

For the fast transient, contribution of the moderator temperature feedback is negligible during the initial part of transient, because the heat transfer rate between the fuel and the moderator is much slower than the neutron flux response. After the initial neutron flux peak, however, the rate of power increase is affected by the moderator temperature feedback. Conservatism required to obtain the maximum peak power and peak heat flux leads the moderator temperature coefficient to the largest value (in positive sense) within the range of possible values that can be reached during the transient.

#### 4.3. Reactor Trip Function

Reactor trips used in this work are the power range high neutron flux trip (low setting and high setting), overpower  $\Delta T$  trip, and overtemperature  $\Delta T$  trip. The most adverse combination of instrument and setpoint errors, delays of trip signal actuation and rod cluster control assembly release is taken into account.

A 10 percent increase is assumed for the power range high neutron flux trip low setpoint, raising it from the nominal value of 25 percent to 35, while a 9 percent increase is for the high setpoint, raising it from the nominal 109 percent to 118. The overpower  $\Delta T$  and overtemperature

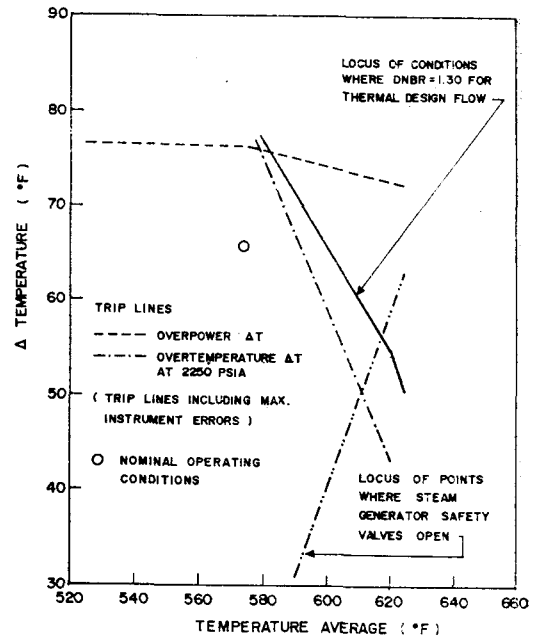


Fig. 2. Overtemperature and Overpower  $\Delta T$  Trip Lines.

$\Delta T$  trip setpoints are shown in Figure 2 as a function of the reactor coolant average temperature at the system pressure of 2250 psia.

For the power range high neutron flux trip, time delay is assumed to be 0.5 seconds from the time that trip conditions are reached to the time at which the rods are free and begin to fall. For the overtemperature  $\Delta T$  and overpower  $\Delta T$  trip, time delay is assumed to be 2.0 seconds.

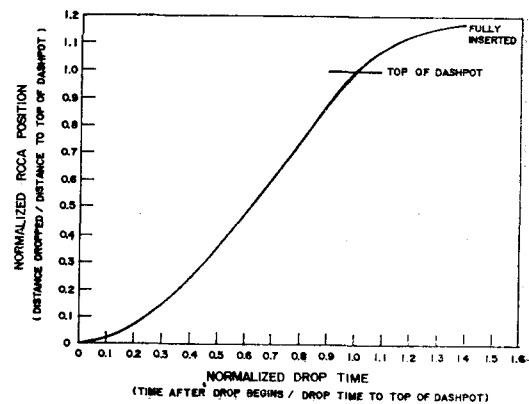


Fig. 3. Rod Cluster Control Assembly Insertion Versus Time after Reactor Trip.

**Table 1. Delayed Neutron Data for Kori Unit 1.**

TIME in LIFE	BOL		MOL		EOL	
DELAYED NEUTRON GROUP	$\beta_{effi}$	$\lambda_i$	$\beta_{effi}$	$\lambda_i$	$\beta_{effi}$	$\lambda_i$
1	0.000228	0.0125	0.000153	0.0126	0.000124	0.0162
2	0.001536	0.0308	0.001097	0.0308	0.000940	0.0307
3	0.001420	0.1155	0.000985	0.1182	0.000832	0.1197
4	0.002966	0.3116	0.002014	0.3165	0.001689	0.3192
5	0.001011	1.2479	0.000707	1.2572	0.000604	1.2586
6	0.000339	3.3531	0.000244	3.3536	0.000211	3.3436
TOTAL FRAC.	0.0075		0.0052		0.0044	
LIFE TIME, $l_p$	18.4 $\mu$ SEC		17.3 $\mu$ SEC		17.9 $\mu$ SEC	

The negative reactivity insertion following a reactor trip is a function of the position versus time of the rod cluster control assemblies and the variation in rod worth as a function of rod position. In the accident analyses, the critical parameter is the time of insertion down to the dashpot entry or approximately 85 percent of the rod cluster travel. In this work, it is conservatively assumed that the insertion time to dashpot entry is 1.8 seconds. The negative reactivity insertion resulting from reactor trip is calculated directly by the one dimensional (axial direction) kinetics code. The rod cluster control assembly position versus time is shown in Figure 3.

#### 4.4. Delayed Neutron Fraction

Typical values for the effective delayed neutron fraction ( $\beta_{eff}$ ) are no less than 0.7 percent at BOL (beginning of life) and 0.5 percent at EOL (end of life) for the initial core. The transients are sensitive to changes in  $\beta_{eff}$  when the inserted reactivity is greater than  $\beta_{eff}$ , since the effective magnitude of reactivity insertion depends on the value of  $\beta_{eff}$ . The power rise for a given reactivity insertion is faster for the small  $\beta_{eff}$ , but the power reduction is also faster after reactor trip. Listed in Table 1 are the six group delayed neutron data at different fuel burnup states employed in the analysis.

#### 4.5. Thermal Parameters

Thermal parameters of pellet and clad are provided as functions of temperature as shown in MATPRO<sup>6)</sup>. The gap conductivity is usually a function of burnup and fission gas pressure. The most conservative value is assumed for this study.

### 5. Sensitivity Analysis

#### 5.1. Uncontrolled Rod Cluster Control Assembly Bank Withdrawal from a Subcritical or Low Power Startup Condition

##### 5.1.1. Reference Case

The first step before performing extensive sensitivity analysis is to select a reference case that provides a basis for various parametric studies. The reference case, herein, is of similar conditions and assumptions to those used for the Kori Unit 1 accident analysis. The basic assumptions and initial conditions used for the reference case are listed in Table 2.

The reactor is assumed to be just critical at hot zero power. This assumption is more conservative than that of a lower initial system temperature. The higher initial system temperature yields the larger heat transfer coefficient and larger specific heat all of which tend to reduce the doppler feedback effect, thereby to

**Table 2. Reference Case Data for Uncontrolled RCCA Bank Withdrawal Accident from Subcritical Condition**

	Conditions
Initial Power Level	$10^{-13}$ to nominal
Burnup State	BOL
Reactivity Insertion Rate	75 PCM/SEC
Effective Delayed Neutron Fraction	0.0075
Coolant Inlet Temperature	547.0 °F
System Pressure	2220 psia
Mass Flow Rate	1 loop running, 8% bypass
Doppler Temperature Coefficient	$-1.6 \times 10^{-5} \Delta k/^\circ F$
Moderator Temperature Coefficient	$0.0 \Delta k/^\circ F$

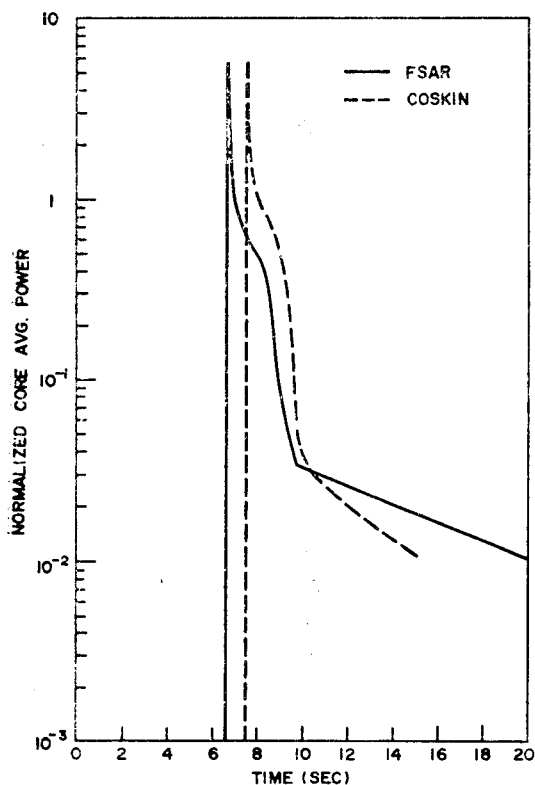


**Fig. 4. Nuclear Power Transient for the RCCA Bank Withdrawal Accident for Subcritical Condition at BOL of Kori Unit 1.**

increase the peak neutron flux. One reactor coolant pump is assumed to be out of service, since the lowest initial coolant flow minimizes the the DNBR.

Calculated results for the reference case are shown in Figure 4 through 6 in comparison with those depicted in the Kori Unit 1 FSAR. Shown in Figure 4 are core average nuclear power transients; one calculated by COSKIN and the other obtained from the FSAR. These results are in good agreement, although the COSKIN predicted time at which the power reaches its maximum is slightly delayed. Such a time delay, however, is not expected to significantly affect the final analysis result since power ramp slopes of the two results are comparable to each other.

Figure 5 shows time dependent core average heat fluxes. From this Figure, the beneficial effect of inherent thermal lag in the fuel is evidenced by a peak heat flux less than the full power nominal value. The minimum DNBR during this transient is not expected to exceed the safety limit. As shown in the Figure, there exists a disagreement between the FSAR result and the present result. However, the FSAR result can not be thought absolutely correct, since a discontinuity of the FSAR heat flux curve at the peak value is not believed physically possible. Such a discontinuity does not exist in the calculation result of the corresponding accident in the Kori Unit 2 FSAR<sup>7)</sup>. It is noted that the calculation for the Kori Unit 2 is performed by the space dependent kinetics code similar to COSKIN, and that its result is of the similar tendency with the COSKIN calculated result. It is suspected that a conservative but simple calculation performed using point kinetics model for FSAR leads to such a discontinuity.

Fuel and clad average temperature transients are shown in Figure 6. The average fuel temperature remains below the nominal full power value. It is noted that the FSAR result shows the higher temperature differential across the fuel pellet compared to the calculated result. It is believed that this is due to the higher fuel

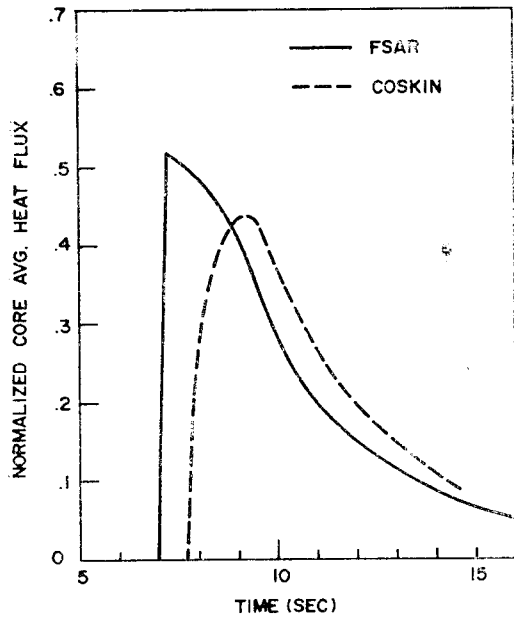


Fig. 5. Core Avg. Heat Flux vs. Time for the RCCA Bank Withdrawal Accident from Subcritical Condition at BOL of Kori Unit 1.

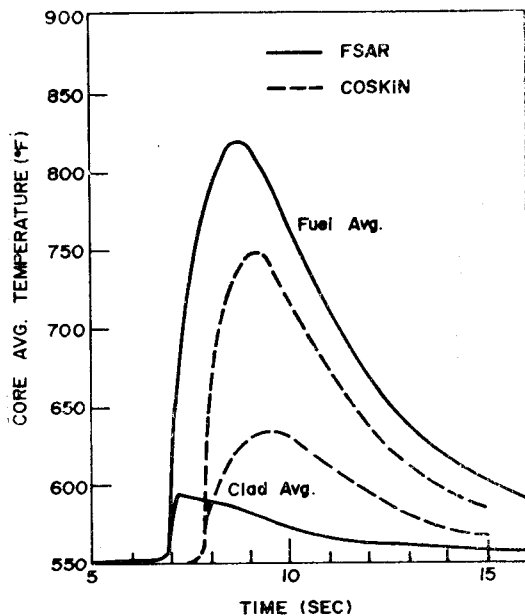


Fig. 6. Fuel and Clad Avg. Temperature vs. Time for the RCCA Bank Withdrawal Accident from Subcritical Condition at BOL of Kori Unit 1.

thermal conductivity assumed in the calculation. It is also recognized that since the energy release and fuel temperature increase during the transient are relatively small, detailed DNBR and hot spot heat transfer calculations are not necessary for the purpose of sensitivity analysis.

As mentioned above, there exist some uncertainties involved in the calculation models and input data. However, they are not expected to significantly affect the validity of the sensitivity analysis due to following reasons. The calculated results are reasonably in good agreement with the FSAR results. And, the sensitivity analysis mainly involves the comparison of the reference case to the case of interest, which reduces the importance of generating correct absolute values.

#### 5.1.2 Parametric Analysis

##### 1) Burnup

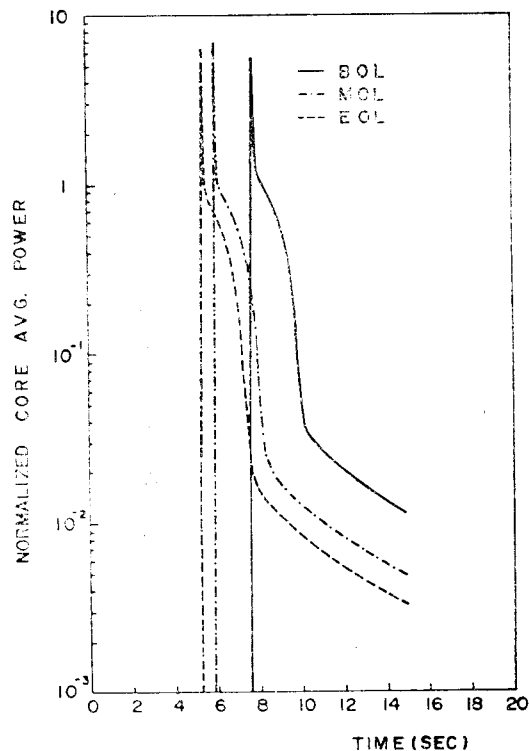


Fig. 7. Neutron Flux Versus Time for the Burnup Sensitivity Test of Uncontrolled Bank Withdrawal Accident from a Subcritical Condition.



As the core burnup progresses core neutron kinetics parameters like delayed neutron fraction and reactivity feedback coefficients are changed. Doppler coefficient does not vary significantly as the burnup progresses, however, moderator temperature coefficient changes considerably. When considering that moderator feedback effects on the core transient behavior are not significant during the fast transient, the most influential

parameter of the above is the delayed neutron fraction,  $\beta_{eff}$ .

As the delayed neutron fraction decreases due to the burnup increase, the elapsed time before the power reaches the peak value is shortened and the reactor trips earlier as shown in Figure 7. Due to the time lag in heat transfer across the fuel pellet, maximum heat flux at the fuel rod surface is higher at EOL resulting in higher fuel temperature as shown in Figure 8. These Figures prove that BOL leads to the most severe transient.

2) Initial Power Level

Shown in Figure 9 are nuclear power transients starting from three different initial power levels;  $10^{-13}$ ,  $10^{-9}$  and  $10^{-5}$  of the nominal power. It is noticed from the Figure that the lowest initial power assumption leads to the high-

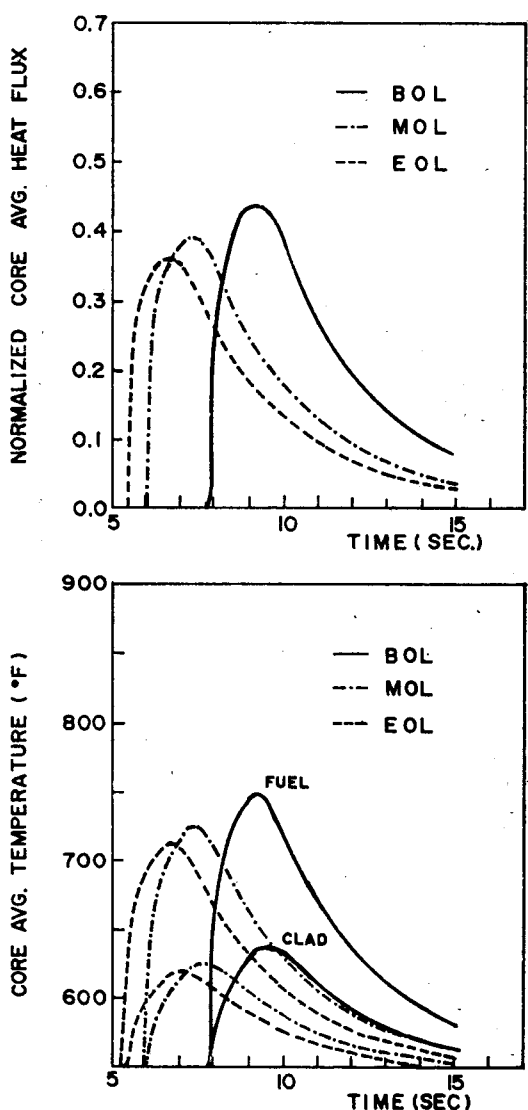


Fig. 8. Thermal Flux vs. Time and Temperature vs. Time for the Burnup Sensitivity Test of Uncontrolled Bank Withdrawal Accident from a Subcritical Condition.

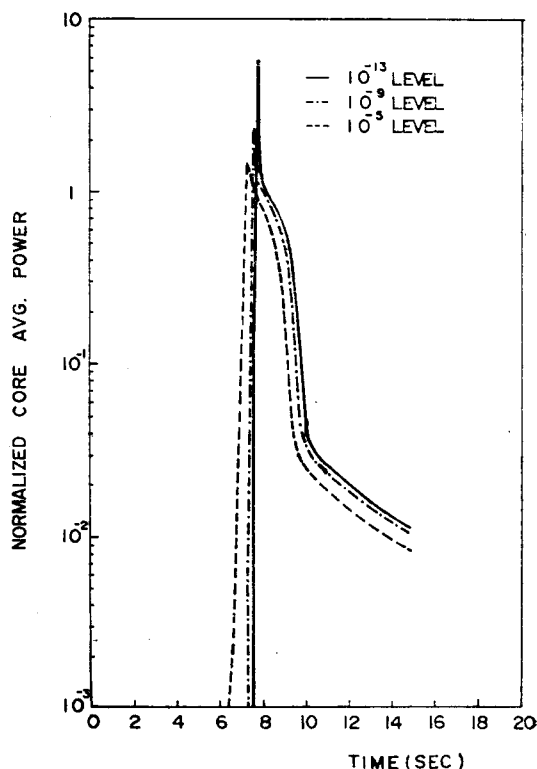


Fig. 9. Neutron Flux Versus Time for the Initial Power Level Sensitivity Test of Uncontrolled Bank Withdrawal from a Subcritical Condition.

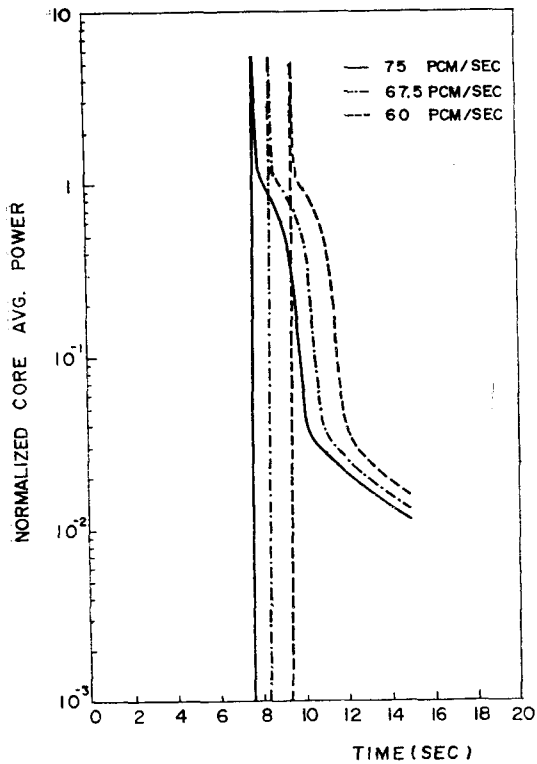


Fig. 10. Neutron Flux Versus Time for the Reactivity Insertion Rate Sensitivity Test of Uncontrolled Bank Withdrawal Accident from a Subcritical Condition.

highest peak power. It is because the power ramp rate is highest for the lowest initial power case when the neutron flux level reaches the power range low flux level trip set point. Therefore, with the higher ramp rate the power level can reach higher point before intrinsic prompt feedback (doppler feedback) takes its effect.

### 3) Reactivity Insertion Rate

It is evident from Figure 10 that the higher the reactivity insertion rate, the higher the peak neutron flux. Therefore, higher reactivity insertion rate assumption will result in more severe accident consequence.

### 4) Coolant Mass Flow Rate

Variation of coolant mass flow rate does not cause significant effect on neutron flux transient. However, it affects the heat removal rate at the fuel rod surface. The less the coolant flow, the

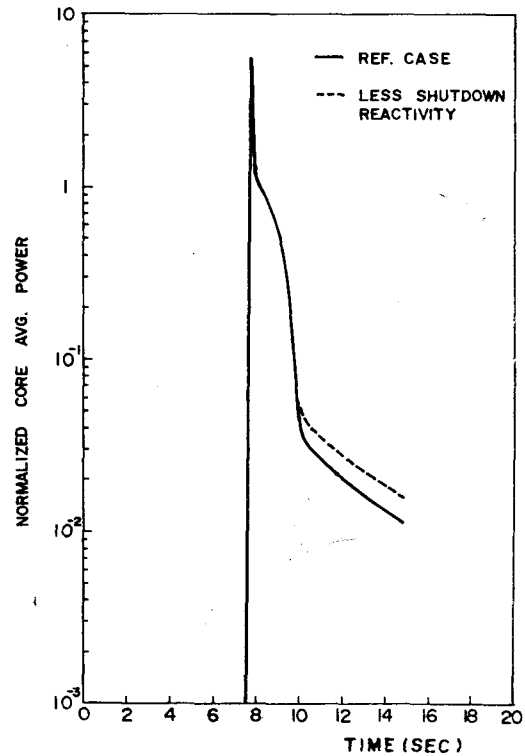


Fig. 11. Neutron Flux Versus Time for the Shutdown Reactivity Sensitivity Test of Uncontrolled Bank Withdrawal Accident for a Subcritical Condition.

higher the fuel rod temperature. The effect of coolant flow rate variation is shown in Table 3.

### 5) Feedback Coefficients

For the reference case calculation, the assumption of minimum feedback coefficients (absolute magnitude) is adopted. If feedback coefficients are larger, the peak power will be lower leading to lower peak heat flux and fuel temperature. As shown in Table 3, the minimum feedback coefficient assumption results in the most severe consequence.

### 6) Shutdown Reactivity

Until control banks are dropped to the dashpot entry, effective shutdown is not fulfilled. As shown in Figure 11, the tail of the transient is higher for the lower shutdown reactivity case leading to slightly higher heat flux and fuel temperature.

**Table 3. Sensitivity Analysis Results of Uncontrolled RCCA Bank Withdrawal Accident from Subcritical Condition (Peak Values of Transient)**

CASE		POWER (% RATED)	HEAT FLUX TO NOMINAL	AVG. FUEL TEMP. (°F)	AVG. CLAD TEMP. (°F)
REFERENCE CASE		586	0.443	750.75	636.83
BURN-UP STATE	MOL	695	0.388	724.44	624.94
	EOL	629	0.361	710.98	618.85
INITIAL POWER LEVEL	10 <sup>-9</sup> LEVEL	230	0.418	738.23	630.77
	10 <sup>-5</sup> LEVEL	147	0.358	710.58	618.44
REACTIVITY INSERTION RATE	-10% RATE	544	0.434	746.40	634.83
	-20% RATE	495	0.426	742.58	633.07
COOLANT MASS FLOW RATE	+10% RATE	586	0.453*	750.23	633.94
	-10% RATE	581	0.433	751.20*	639.96*
MAX. FEEDBACK COEFFICIENT		435	0.297	683.52	607.53
LESS SHUTDOWN REACTIVITY		586	0.445*	751.85*	639.96*

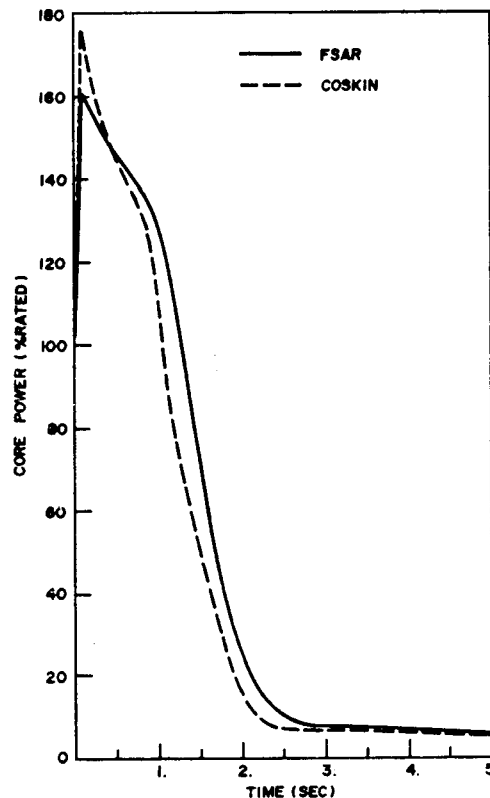
\*Value larger than that of the reference case

**Table 4. Parameters Used in the Analysis of the Rod Ejection Accidents**

Time in Life Power Level	BOL	BOL	EOL	EOL
	102%	0%	102%	0%
Ejected rod worth % $\Delta K$	0.20	0.83	0.20	1.02
Delayed neutron fraction %	0.52	0.52	0.44	0.44
Feedback reactivity weighting	1.30	2.0	1.20	2.30
F <sub>Q</sub> before rod ejection	2.51	—	2.51	—
F <sub>Q</sub> after rod ejection	6.13	10.10	4.23	15.10
Number of operating pumps	2	1	2	1

### 5.1.3 Discussion on Analysis Results

Summarized in Table 3 are the overall sensitivity analysis results on uncontrolled rod cluster control assembly bank withdrawal accident from a subcritical or low power startup condition. The most severe is found to be the case of BOL at maximum reactivity insertion rate from the lower level with minimum feedback coefficients, minimum coolant mass flow rate and minimum shutdown reactivity available. Through the sensitivity analysis the assumptions and initial conditions from FSAR for the analysis of Kori Unit 1 control bank withdrawal accident are found most conservative and limiting.

**Fig. 12. Nuclear Power Transient for the Rod Ejection Accident at HFP-BOL.**

5.2 Rod Ejection Accident

5.2.1. Reference Case

The selected reference case for the sensitivity analysis on Kori Unit 1 rod ejection accident is the accident occurring at HFP (hot full power) and BOL. Parameters used for the analysis of the reference case are listed in Table 4 along with those for other cases. The ejected rod worth and hot channel factors are calculated by 2D/1D synthesis method<sup>8)</sup>.

Shown in Figure 12 are the nuclear power transients for the reference case; one is calculated by COSKIN and the other is obtained from the FSAR. Two curves are reasonably in good agreement, although the COSKIN calculation predicts the higher peak power compared to the FSAR.

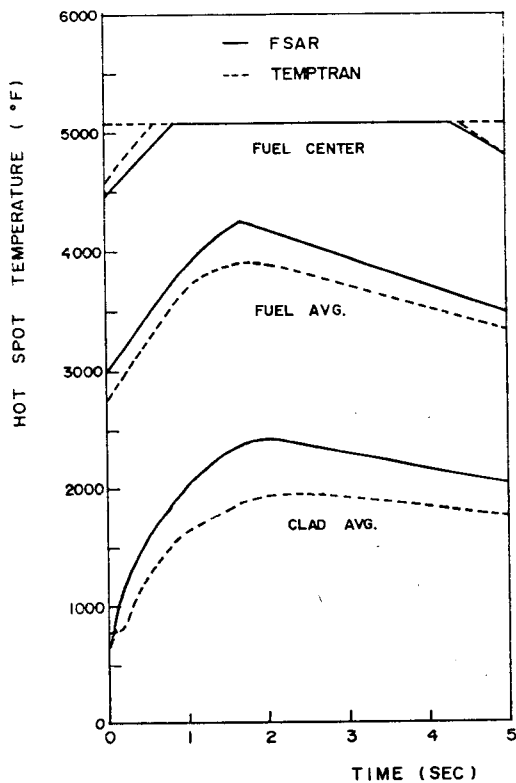


Fig. 13. Hot Spot Fuel and Clad Temperature Versus Time for the Rod Ejection Accident at HFP-BOL.

Figure 13 compares the hot spot temperature calculation results obtained from the TEMPTRAN calculation to those from the FSAR, respectively. These are also in good agreement. As shown in the Figure the fuel centerline experiences some melting for a short period.

Here, it is of interest to observe the variation of axial peaking factor during the transient predicted by the COSKIN code. Figure 14 shows both the core average power change and variation of axial peaking factor in time. The maximum in the axial peaking factor occurs at 1.9 sec by

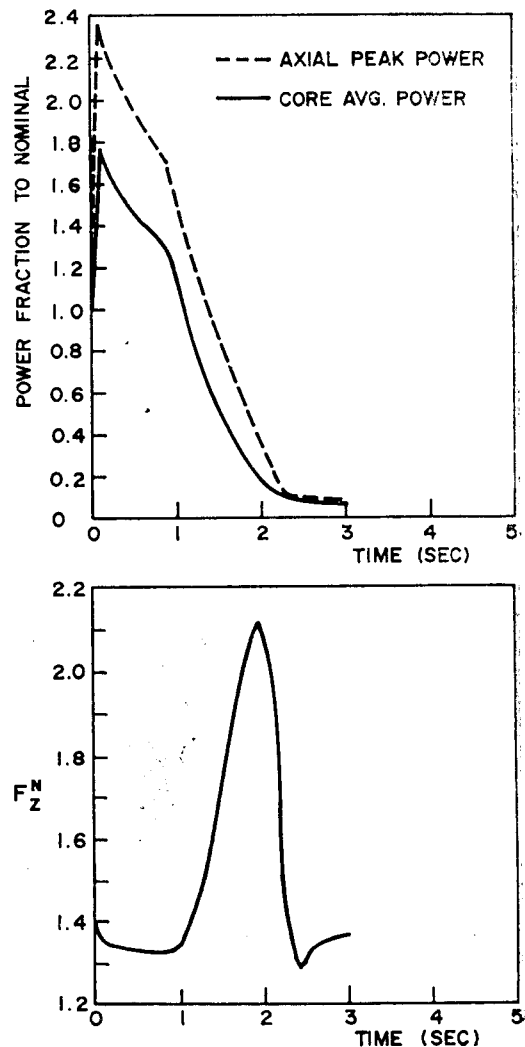


Fig. 14. Axial Peaking Factor,  $F^{Nz}$ , Versus Time for the Rod Ejection Accident at HFP-BOL.

the movement of control banks. Figure 15 shows axial power shape versus time for the reference case.

### 5.2.2. Parametric Analysis

#### 1) Burnup and Power Level

Rod ejection accident is analyzed for both BOL and EOL from zero and full power initial condition. Assumptions and initial conditions for these four cases are summarized in Table 4, that are obtained from the Kori Unit 1 FSAR. Figures 16 and 17 show nuclear power transients for the above mentioned four cases. Results of the hot spot heat transfer calculations are also summarized in Table 5.

As the burnup increases,  $\beta_{\text{eff}}$  becomes smaller. Due to the smaller  $\beta_{\text{eff}}$  at EOL, reactor power for a given reactivity input rises and drops more rapidly than at BOL following the reactor trip. In the case of 102% initial power, the peak power during the transient is slightly higher at EOL as shown in Figure 16. However, due to

the better heat transfer between the fuel and the coolant, the centerline fuel temperature as well as the stored energy is lower at EOL.

In the case of zero initial power, calculated ejected rod worth and  $F_q$  (hot channel factor) after rod ejection are higher at EOL. As shown in Figure 17, the core average power transient at BOL is close to that at EOL. However, due to the higher peaking factor, maximum fuel centerline temperature and stored energy in the fuel are higher at EOL. From Table 5 it is generally deduced that the HFP-BOL case leads to the most severe result among four cases as far as fuel centerline temperature and stored energy are concerned. But, HZP-EOL case results in the highest clad temperature. This is due

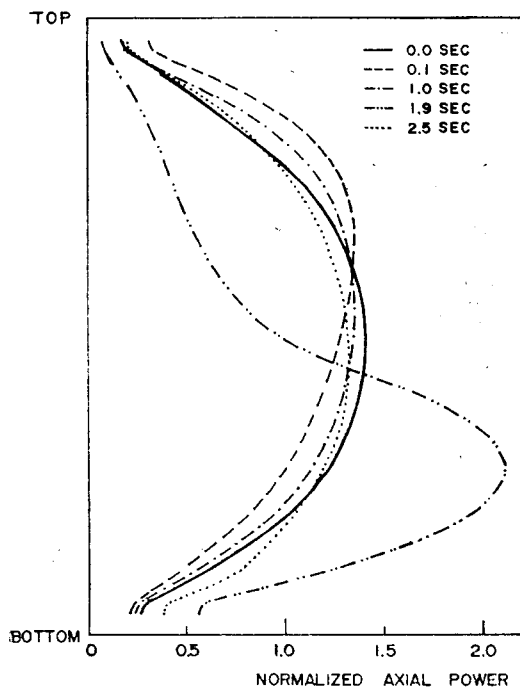


Fig. 15. Axial Power Shape vs. Time for the Rod Ejection Accident at HFP-BOL.

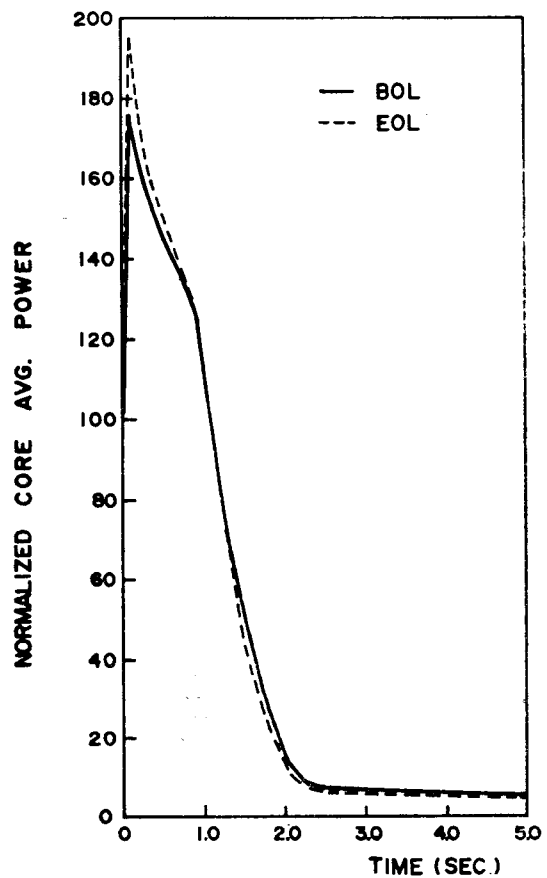


Fig. 16. Nuclear Power Transient for the Burnup Sensitivity Test of Rod Ejection Accident at HFP.

**Table 5. Results of the Hot Spot Heat Transfer Calculation for Rod Ejection Accident**

Time in Life Power Level	BOL 102%	EOL 102%	BOL 0%	EOL 0%
Max. Fuel Centerline Temperature, °F	5,080*	4,174	3,170	3,988
	5,080*	4,709	2,886	3,883
Max. Fuel Average Temperature, °F		+12.8%	-9.0%	-2.6%
	4,228*	2,978	2,745	3,504
Max. Clad Temperature, °F	3,919*	3,237	2,487	3,248
	-7.3%	+8.7%	-9.4%	-7.3%
Max. Fuel Stored Energy, Cal/gm	2,460	1,718	2,030	2,624*
	1,978	1,773	1,859	2,337*
Max. Fuel Stored Energy, Cal/gm		+3.2%	18.4%	-10.9%
	186.5*	123.0	112.0	149.0
	169.6*	135.1	99.2	135.7
	-9.1%	+9.8%	-11.4%	-8.9%

\* Maximum value among the four cases.

FSAR  
CALCULATED  
DIFFERENCE

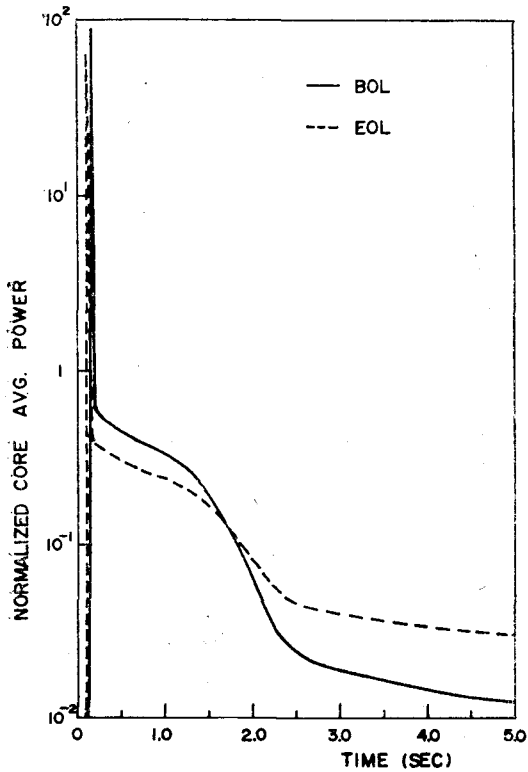


**Fig. 17. Nuclear Power Transient for the Burnup Sensitivity Test of Rod Ejection Accident at HZP.**

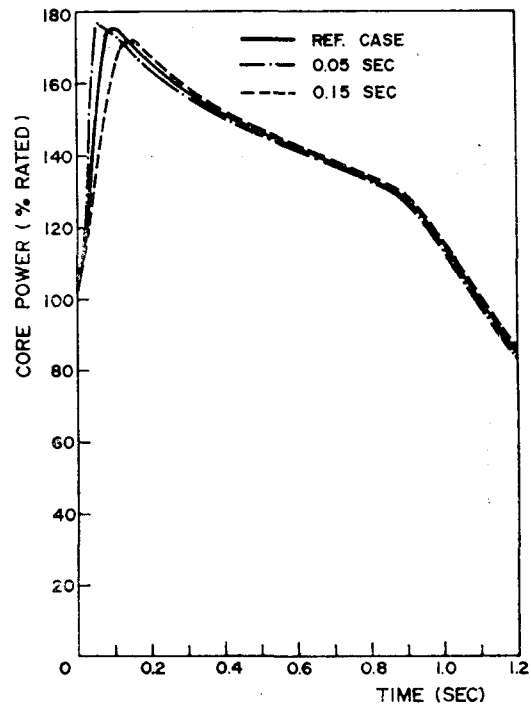


**Fig. 18. Nuclear Power Transient for the Rod Ejection Time Sensitivity Test of Rod Ejection Accident at HFP-BOL.**

to several combined effects such as higher ejected rod worth, higher  $F_Q$  after rod ejection, and lower coolant flow rate compared to the HFP-BOL case.

#### 2) Rod Ejection Time

For the reference case, the time required for the rod to be fully ejected is assumed to be 0.1 seconds. For comparison purpose, two other values for rod ejection time (0.05 and 0.15 seconds) are considered, and the comparison results are shown in Figure 18. The rod ejection time is not found to significantly affect the transient.

#### 3) Doppler Weighting Factor

For the fast transient, doppler effect plays the most important role as a prompt intrinsic feedback in limiting the power excursion. The concept of doppler weighting factor is adopted to compensate for the deficiencies from non-three dimensional calculation. The local power at hot channel is higher than that at an average channel, and that leads to higher fuel temperature and larger doppler feedback. The weighting factor as a function of local neutron flux should be increased at hot channel compared to that for the average channel. Since the COSKIN code, the one dimensional calculation code in axial direction, is of the assumption of radially uniform core characteristics, non-uniformity of radial neutron flux should be taken into account utilizing the doppler weighting factor.

It is noted that the calculation results are sensitive to the changes in weighting factor. The smaller doppler weighting factor leads to the higher peak power and higher hot spot fuel temperature.

#### 4) Coolant Mass Flow Rate

Small Change in the coolant flow rate from the reference value barely affects the nuclear power transient. Also, the peak transient fuel temperature is not changed significantly, because the transient is rapid and heat transfer is nearly

adiabatic. However, due to poorer heat transfer from the clad to the coolant under reduced flow condition, the peak clad temperature becomes slightly higher.

#### 5) Thermal Parameters

Five percent variation is examined in the gap heat transfer coefficient and the fuel thermal conductivity. The transient is moderately sensitive to the variation of these parameters. As expected at lower conductivity, more energy is stored in the fuel and the fuel temperature rise is higher.

#### 6) Hot Channel Factor ( $F_Q$ )

Since the hot spot transient is obtained by multiplying the average channel transient by the hot channel factor,  $F_Q$  the severity of the hot spot enthalpy rise increases in proportion to the increase in  $F_Q$ . The higher the hot channel factor, the more the stored energy in the fuel leading to the higher hot spot temperature.

#### 5.2.3. Discussion on Analysis Results

The overall sensitivity analysis results on the Kori Unit 1 rod ejection accidents are summarized in Table 6. Among the parameters of interest the most sensitive is the doppler weighting factor. At BOL the most severe accident consequence results from the assumption of full power initial condition, lowest doppler weighting factor, lowest mass flow rate, worst thermal conduction and highest hot channel factor.

Due to the fact that the HZP-EOL case leads to the highest clad temperature while the HFP-BOL case results in the highest fuel stored energy and centerline temperature, no single case can be selected as a limiting case for the rod ejection accident. Therefore, it is reasonable to consider four different cases (HFP-BOL, HFP-EOL, HZP-BOL, and HZP-EOL) in FSAR to envelope the most limiting case.

## 6. Conclusion

It is not easy to draw a general conclusion

Table 6. Sensitivity Analysis Results of Rod Ejection Accident for HFP-BOL (Peak Values)

CASE		CORE AVG. POWER (% RATED)	HOT SPOT FUEL CENTER TEMP. (°F)	HOT SPOT FUEL AVG. TEMP. (°F)	HOT SPOT CLADD- ING TEMP. (°F)	HOT SPOT FUEL STORED ENERGY (Cal/gm)
REFERENCE CASE		175.6	>5,080	3,919	1,978	169.6
EJECTION TIME	0.05 SEC.	176.5*	>5,080	3,919	1,975	169.6
	0.15 SEC.	172.5	>5,080	3,914	1,979*	169.3
DOPPLER WEIGHTING	+5%	133.4	~5,080	3,685	1,851	157.6
	-5%	251.0**	>5,080	4,169**	2,136**	182.7**
COOLANT MASS FLOW RATE	+5% RATE	175.6	>5,080	3,889	1,952	168.1
	-5% RATE	175.5	>5,080	3,924*	2,006	169.8*
THERMAL CONDUCTANCE	5% BETIER		~5,080	3,809	1,975	163.9
	5% WORSE		>5,080	4,036*	1,984*	175.6*
HOT CHANNEL FACTOR	+5%		>5,080	3,972*	2,026*	172.3*
	-5%		>5,080	3,852	1,931	166.1

\* Value larger than that of the reference case.

\*\* Largest value.

from the sensitivity analysis on the reactivity induced accidents. However, for relatively fast transients as studied in this paper, low coolant mass flow rate and low feedback assumptions are proven to be conservative. Also, such accidents occurring at BOL are usually more limiting than those occurring at EOL. For DNBR calculation, higher fuel thermal conductivity assumption is more conservative, while lower conductivity assumption is more conservative for centerline fuel temperature calculation.

Through the sensitivity study performed herein, an insight has been gained into the reactor core transient behavior during the relatively fast reactivity induced accidents. The computer codes developed or adapted for the analysis are evaluated to be reliable, especially for sensitivity analysis, while there is still a room for further improvement.

### References

1. "Final Safety Analysis Report for Kori Nuclear Power Plant Unit No. 1," Korea Electric Company (1976).
2. G. Forti, "COSTAX-BoIL—A Computer Programme of the COSTANZA Series for the Axial Dynamics of BWR and PWR Nuclear Reactors," EUR 4497e (1970).
3. Myung Hyun Kim, "User's Manual of TEMPT-RAN—A Fortran IV Code for Thermal Transients in a UO<sub>2</sub> Fuel Rod," Korea Advanced Energy Research Institute, to be published, (1982).
4. H.G. Hargrove, "FACTRAN—A Fortran IV Code for Thermal Transients in a UO<sub>2</sub> Fuel Rod," WCAP-7908, (1972).
5. Hyun Koon Kim, "User's Guide of SCAN—One-Dimensional Single Channel Thermal-Hydraulic Departure from Nucleate Boiling Analysis Code," Korea Advanced Energy Research Institute, to be published (1982).
6. "MATPRO-VERSION 10, A Handbook of Material Properties for Use in the Analysis of Light Water Reactor Fuel Rod Behavior," TREE-NUREG-1180, EG & G Idaho (1978).
7. "Final Safety Analysis Report for Kori Nuclear Power Plant Unit No. 2," Korea Electric Company (1981).
8. T. Morita et al., "Power Distribution Control and Load Following Procedures," WCAP-8403 (1974).